Environmental Science & Technology

Article

pubs.acs.org/est

Olivine Dissolution in Seawater: Implications for CO_2 Sequestration through Enhanced Weathering in Coastal Environments

Francesc Montserrat,[*,†] Phil Renforth,[‡] Jens Hartmann,[§] Martine Leermakers,[†] Pol Knops,[∥] and Filip J. R. Meysman[†,⊥,#]

[†]Department of Analytical, Environmental and Geo-Chemistry, Free University of Brussels, Pleinlaan 2, 1050 Brussels, Belgium

[‡]School of Earth and Ocean Sciences, Cardiff University, Main Building, Park Place, Cardiff, CF10 3AT United Kingdom

[§]Institute for Geology, Center for Earth System research and sustainability (CEN), Universität Hamburg, Bundesstraße 55, 20146 Hamburg, Germany

[∥]Green Minerals B.V., Boulevard 17, 6127 AX Grevenbicht, The Netherlands

[⊥]Aarhus Institute of Advanced Studies (AIAS), Aarhus University, Hoegh-Guldbergs Gade 6B, DK-8000 Aarhus C, Denmark

[#]NIOZ Royal Netherlands Institute for Sea Research, Department of Estuarine and Delta Systems, and Utrecht University, Korringaweg 7, 4401 NT Yerseke, The Netherlands

Supporting Information

ABSTRACT: Enhanced weathering of (ultra)basic silicate rocks such as olivine-rich dunite has been proposed as a large-scale climate engineering approach. When implemented in coastal environments, olivine weathering is expected to increase seawater alkalinity, thus resulting in additional CO_2 uptake from the atmosphere. However, the mechanisms of marine olivine weathering and its effect on seawater–carbonate chemistry remain poorly understood. Here, we present results from batch reaction experiments, in which forsteritic olivine was subjected to rotational agitation in different seawater media for periods of days to months. Olivine dissolution caused a significant increase in alkalinity of the seawater with a consequent DIC increase due to CO_2 invasion, thus confirming viability of the basic concept of enhanced silicate weathering. However, our experiments also identified several important challenges with respect to the detailed quantification of the CO_2 sequestration efficiency under field conditions, which include nonstoichiometric dissolution, potential pore water saturation in the seabed, and the potential occurrence of secondary reactions. Before enhanced weathering of olivine in coastal environments can be considered an option for realizing negative CO_2 emissions for climate mitigation purposes, these aspects need further experimental assessment.

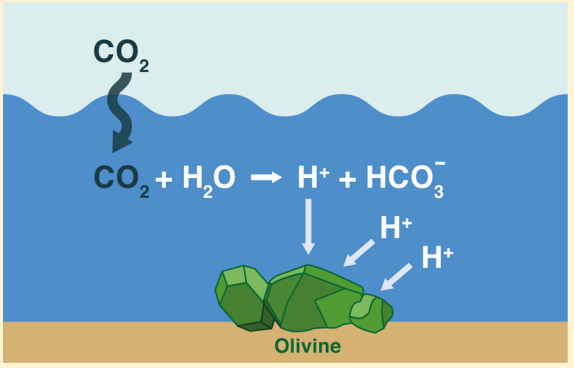

INTRODUCTION

Climate engineering approaches that aim to deliberately and actively remove greenhouse gases from the atmosphere are categorized as carbon dioxide removal (CDR) or negative emission technologies (NETs).[1] CDR or NETs are seen as a possible future complement to current climate policies, which are presently only focused on the reduction of CO_2 emissions. Model studies emphasize that the large-scale implementation of NETs will be needed to limit global warming to within a 2 °C increase with respect to preindustrial conditions.[2,3] The worldwide commitment to attain this target, thus avoiding a "dangerous" level of climate change, has been strengthened by the recent COP21 Paris Agreement.[4]

Enhanced silicate weathering (ESW) is a NET approach in which the natural process of (silicate) rock weathering is artificially stimulated.[5,6] The technique has been recognized as a potentially promising strategy for CO_2 removal from the atmosphere while at the same time counteracting ocean acidification.[1,6−9] The implementation of ESW requires suitable source rock to be mined, ground to small grain sizes, and subsequently spread over suitable areas.[5] The mineral grains dissolve (i.e., chemical weathering), through which CO_2 is eventually captured from the atmosphere.[6,10] Olivine ($Mg_{2-x}Fe_xSiO_4$) is an abundant and fast-weathering ultramafic silicate mineral and has been advanced as a prime candidate mineral for ESW application.[5,11] The dissolution of olivine in an aqueous environment consumes protons or equally increases alkalinity,[6,12,13] and so increases CO_2 uptake by the aqueous medium (Supporting Information section 1).

In theory, ESW can be applied in terrestrial soils,[5,6] in the surface mixed layer of the open ocean,[13] or by spreading

Received: November 24, 2016
Revised: March 9, 2017
Accepted: March 10, 2017
Published: March 10, 2017

DOI: 10.1021/acs.est.6b05942
Environ. Sci. Technol. 2017, 51, 3960−3972

minerals onto sediments of the coastal zone and continental shelf.[14] The largest application domain for ESW would be the open ocean, but model analysis suggests that the olivine particles need to be ground to very small sizes to facilitate dissolution in the surface ocean.[13] As such, the high grinding costs and CO_2 emissions during production potentially limit this approach. An alternative scheme is the application of ESW to coastal and shelf environments, where it could be integrated into existing coastal zone management practices, such as dredging operations, land reclamation, and beach nourishment. A theoretical examination of the concept of coastal ESW[14] has indicated advantages as well as challenges. One important knowledge gap is that detailed experimental investigations of olivine dissolution under natural conditions (i.e., realistic for coastal ESW) are lacking. A better understanding of the rate and mechanism of olivine dissolution in natural marine environments is needed to better evaluate the feasibility and potential of coastal ESW as a NET. Previous work has largely focused on olivine dissolution under laboratory conditions using artificial seawater solutions.[15−18] Such idealized approaches potentially exclude important geochemical and environmental influences that could be relevant under field conditions.

Here, we specifically address a number of questions related to the application of enhanced silicate weathering in natural coastal environments: (1) What is the rate of olivine dissolution in natural seawater and how does this differ from artificial seawater? (2) Does olivine dissolve stoichiometrically in natural seawater? (3) What dissolution products can be used to efficiently monitor the dissolution rate of olivine in coastal sediments, i.e., quantify the efficiency of enhanced silicate weathering? (4) To what extent does secondary mineral formation diminish the CO_2 sequestration efficiency of olivine dissolution in seawater?

We present results from dissolution experiments with simulated grain−grain collisions, in which olivine was dissolved in natural filtered seawater as well as in artificial seawater media with modified cation composition. Potential proxies for quantifying the dissolution rate of olivine are analyzed and compared. Based on these results, we discuss a number of challenges for ESW in coastal environments.

MATERIALS AND METHODS

Materials. Commercially available olivine sand ($Mg_{2-x}Fe_xSiO_4$) and lab-grade quartz (SiO_2) were used in slurry dissolution experiments. The olivine sand (particle size quantiles: D10 = 91 μm, D50 = 143 μm, D90 = 224 μm) had a molar Mg-to-Fe ratio of 0.94:0.06, characterizing the olivine as forsterite-94 (Fo_{94}). The Ni content was estimated at 0.0075 mol Ni mol^{-1} olivine. Further details on the chemical composition, grain-size distribution, and pre-experimental treatment are summarized in Tables S1 and S2.

Different reactive seawater media were used as supernatant. Filtered seawater (FSW) was collected as natural seawater from the Oosterschelde tidal basin (The Netherlands) and filtered over a Mahle amaGuard FP 0.2 [μm] woven cotton filter (Mahle Benelux, The Netherlands). In addition, three types of artificial seawater were prepared according to the ASTM Standard Practice D 1141−98[19] (Table S3): (1) plain artificial seawater (ASW), (2) artificial seawater with Ca^{2+} replaced by Na^+ (hereafter named ASW-Ca), and (3) artificial seawater with both Ca^{2+} and Mg^{2+} replaced by Na^+ (hereafter named ASW-CaMg).

Experiments. Specific amounts of olivine and quartz grains were added to a specific volume of seawater in 500 mL borosilicate glass bottles, which were then subjected to continuous rotating movements on a CH-4103 rotating shaking platform (INFORS AG, Switzerland) set at 155 rpm. The bottles were closed with membrane screw caps, equipped with a 0.5 mm thick silicone septum that prevented evaporation but allowed gas exchange. To prevent photosynthesis, the experiment took place in the dark, while the bottles were wrapped in aluminum foil (leaving the top of the membrane cap uncovered).

A total of three types of agitation experiments were conducted: A1, A2, and A3 (Supporting Information section 3 and Table S4). In both the A1 and A2 experiments, 0.1 mol of either olivine (OLI) or quartz (QUA) were added to 300 mL of FSW, with one control treatment (i.e., only seawater; SW). A total of three replicates were conducted per treatment (n = 3). Experiment A1 was conducted under ambient conditions, i.e. without regulation of temperature (range: 13.5−20 °C) and pCO_2 (range: 445−525 ppmv), and lasted for 88 days. The second agitation experiment, A2, had essentially the same setup as A1 except for a few modifications. First, natural seawater was bubbled with air prior to the experiment to ensure CO_2 equilibration with the surrounding atmosphere. Second, the experiment had a much shorter duration (20 days), and it was conducted under stable temperature and pCO_2 conditions. The third experiment, A3, was designed to specifically investigate the effect of the composition of seawater on the dissolution rate of olivine (quartz was not investigated). Agitation experiment A3 was designed to examine the effect of the composition of seawater on the dissolution rate. A3 was also conducted under stable temperature and pCO_2 conditions and used atmosphere-equilibrated reactive fluids, bubbled with air. The dissolution of olivine (OLI) was monitored in four reactive fluids (FSW, ASW, ASW-Ca, and ASW-CaMg; see the Supporting Information section 2) and compared to control treatments (respective solution media without olivine). Instead of 0.10 mol olivine used in A1 and A2, and 0.03 mol was used in A3 (Table S3).

To test the impact of agitation, a layer of olivine sand was placed also in a nonmoving cylindrical container with FSW (n = 1). In this nonagitated treatment, the olivine itself was not agitated. Rather, the overlying water was stirred, and only samples for solid-phase analysis were collected.

Water and Solid-Phase Analysis. The overlying water of the slurry batch reaction experiments was sampled at regular time intervals and analyzed for temperature, salinity, pH, total alkalinity (TA), dissolved inorganic carbon (DIC), dissolved silicate (Si), dissolved nickel (Ni), and dissolved magnesium (Mg) using standard analytical procedures[20,21] (see section 3 of the Supporting Information). All solute concentrations are reported as μmol per kg of seawater (μmol kg^{-1}).

Upon completion of the A3 experiment, olivine grains were recovered from the agitated and nonagitated treatments, inspected for dissolution features, and analyzed for carbonate precipitates, according to Nieuwenhuize et al.,[20] to yield the mass percentage of inorganic carbon (mass% C_{inorg}). The elemental composition of the olivine particle surfaces were investigated using scanning electron microscope energy-dispersive X-ray spectroscopy (SEM−EDX). Additional details on both water and solid-phase analyses can be found in section 3 of the Supporting Information.

DOI: 10.1021/acs.est.6b05942
Environ. Sci. Technol. 2017, 51, 3960−3972

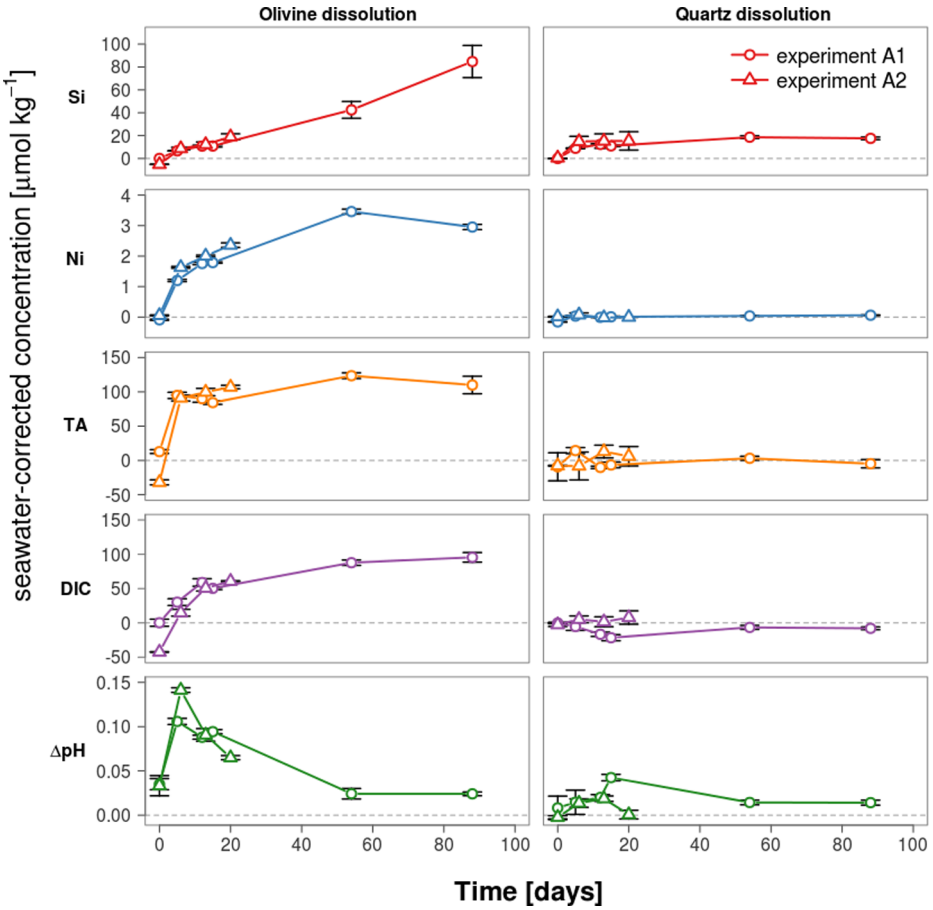

Figure 1. Temporal development of olivine dissolution response variables in experiments A1 and A2. Symbols denote mean seawater-corrected values (see the Materials and Methods section), with error bars denoting standard error of the mean (SEM). Circles: values from experiment A1; triangles: values from experiment A2. The values for both experiments are plotted with the olivine (OLI) and quartz (QUA) treatments plotted alongside on the same vertical scale for comparison. The reported units are μmol/kg of seawater, except for pH, which is in pH units on the total scale.

Olivine Dissolution Rate Calculations and Simulations. The accumulation over time of the reaction products in the reactor vessels is reported as excess concentration values, $\Delta C_i(t) = C_{treatment}(t) - C_{control}(t)$. In this, the control refers to the treatment without the addition of any solid minerals. A total of three empirical mathematical models were implemented to describe $\Delta C_i(t)$ as a function of the incubation time, and from these model fits, the accumulation rate R_i [μmol kg^{-1} day^{-1}] of compound i and the associated area-specific dissolution rate constant k_i [μmol m^{-2} day^{-1}] were derived (section 4 of the Supporting Information). Note that in the case of stoichiometric dissolution, the rate constants k_i should be, at least in theory, identical for all olivine dissolution products.

The accumulation of weathering products and the change of solution chemistry during the batch dissolution experiments was also mechanistically simulated using the geochemical software package PHREEQC v2[22]. In these simulations, the solution chemistry (and, hence, the saturation states) were free to evolve with time as a consequence of mineral dissolution (kinetic rate equations specified in section 4 of the Supporting Information). Solubility constants were taken from the MINTEQ.dat and LLNL.dat databases to calculate the saturation states of solid phases in the solution. The measured initial composition of the solution, which was specific for each treatment, was used as the starting conditions for the PHREEQC simulations.

All mathematical analyses, apart from the PHREEQC analyses, and plotting were done using the open source R framework for statistical computing.[23]

RESULTS

Olivine and Quartz Dissolution in Natural Filtered Seawater. In the A1 and A2 experiments, we investigated the dissolution of olivine and quartz in natural filtered seawater. In both A1 and A2, there was a clear ΔSi signal in the quartz treatment (QUA), most likely caused by dissolution of very fine quartz particles (Figure 1). ΔSi increased until ~18 μmol kg^{-1} within the first week of the experiments, after which it remained constant. There was no discernible Ni release in the A1 and A2 quartz treatment (Figure 1), and hardly any response from the carbonate system. The ΔpH increased by 0.05 within the first 2 weeks but then decreased again to its initial value by the end of the experiment. While ΔTA remained constant with time, ΔDIC decreased with 22 μmol kg^{-1} during the first 15 days, likely caused by CO_2 outgassing, as the initial solution in A1 may not have been in equilibrium with the atmosphere (sections 2 and 3 of the Supporting Information). In the A2 experiment, the experimental procedure was improved, and the FSW medium was bubbled with ambient air at the start of the experiment. As a result, the carbonate system variables ΔDIC, ΔTA, or ΔpH did not change significantly over time (linear regression, $p = 0.35$, $p = 0.28$, and $p = 0.696$, respectively).

DOI: 10.1021/acs.est.6b05942
Environ. Sci. Technol. 2017, 51, 3960−3972

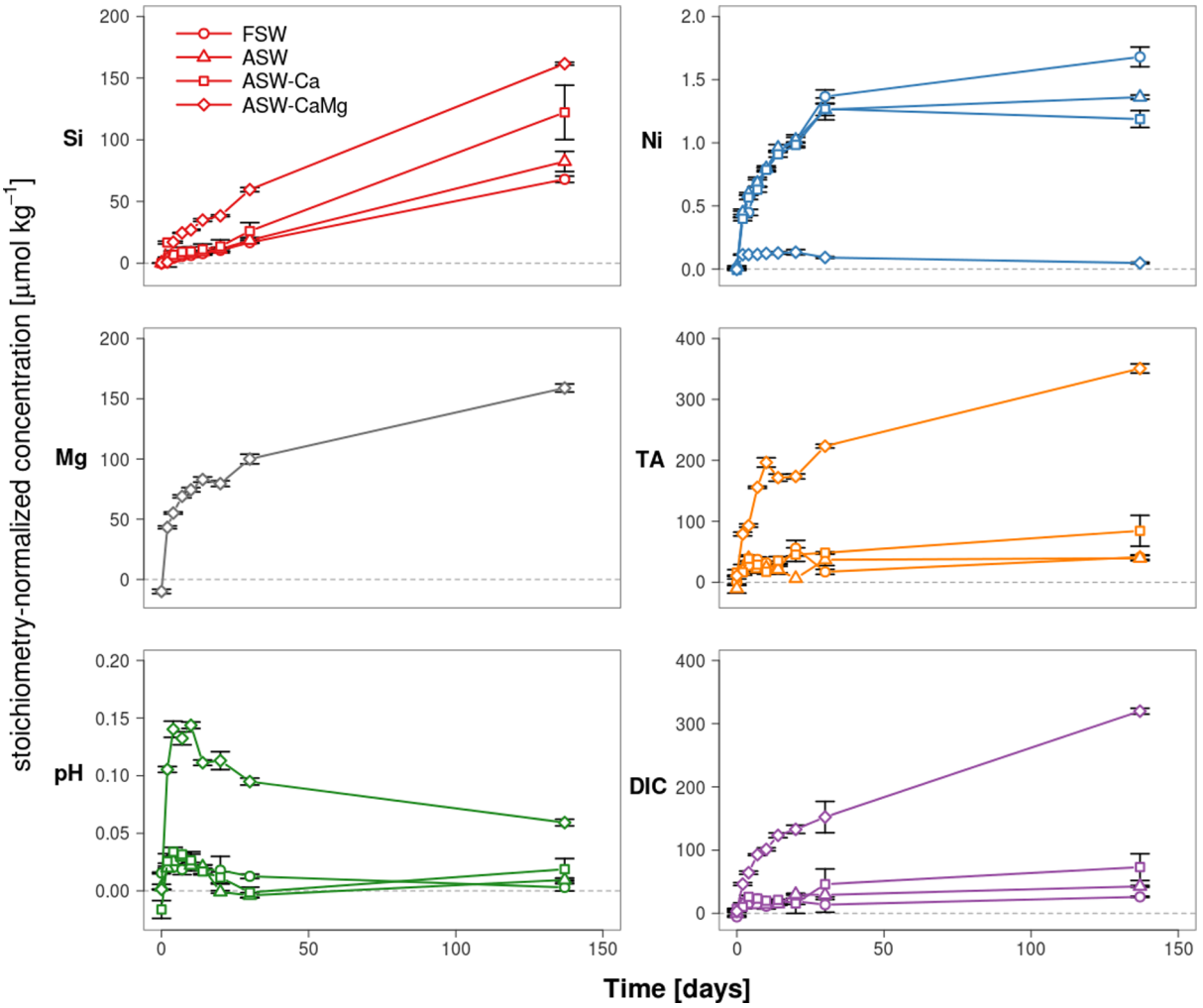

Figure 2. Temporal development of olivine dissolution response variables in experiment A3. Symbols denote mean seawater-corrected values (see the Materials and Methods section) for the olivine treatment (OLI), with error bars denoting standard error of the mean (SEM). Circles: values from filtered seawater treatment (FSW); triangles: values from artificial seawater treatment (ASW); squares: values from artificial seawater without calcium treatment (ASW-Ca); diamonds: values from artificial seawater without calcium and magnesium treatment (ASW-CaMg). The reported units are μmol/kg of seawater (corrected for control values), except for pH, which is in pH units on the Total scale.

In the olivine treatment (OLI) of experiment A1, increases with time of both ΔSi and ΔNi were observed, suggesting olivine dissolution (Figure 1). While ΔNi leveled off at 3.2 μmol kg^{-1}, suggesting that an equilibrium was reached, ΔSi increased almost linearly over the 88 day incubation period, displaying a much-stronger dissolution than in the QUA treatment. Experiment A2 showed a similar temporal evolution of ΔSi and ΔNi (Figure 1). ΔTA showed a pronounced increase over the first 5 days (Figure 1), leveling off thereafter at ΔTA = 103 μmol kg^{-1}. ΔDIC increased in a similar way, albeit over a slightly longer period of ∼15 days, leveling off at ΔDIC = 93 μmol kg^{-1}. The pH in the olivine treatment increased rapidly over the first 5 days by ∼0.1, after which it decreased again and leveled off at ΔpH = 0.02 (Figure 1). The carbonate system in A2 showed a similar pattern, with ΔTA and ΔDIC leveling off at 104 and 74 μmol kg^{-1}, respectively (Figure 1). Similar to experiment A1, the ΔpH in A2 increased strongly within the first 6 days by ∼0.15, after which it decreased again to ΔpH = 0.06 (Figure 1).

Olivine Dissolution in Artificial Seawater Media with Different Cation Composition. In experiment A3, large differences in the release of dissolution products were observed between the different seawater media. All four media displayed a quasi-linear ΔSi response with time (Figure 2). The ΔSi attained at the end of the experiment was lowest in the natural seawater (FSW: 68 μmol Si kg^{-1}) and artificial seawater (ASW: 82 μmol Si kg^{-1}) and increased markedly when Ca^{2+} and Mg^{2+} were replaced by Na^{+} in the medium (ASW-Ca: 122 μmol Si kg^{-1}; ASW-CaMg: 162 μmol Si kg^{-1}).

The Ni release showed a saturation-type response, which varied between media. In the FSW, ASW, and ASW-Ca treatments (Figure 2), the ΔNi concentration showed a comparable accumulation (plateau concentrations between 1.19 and 1.68 μmol Ni kg^{-1}). In contrast, the ASW-CaMg treatment showed hardly any Ni accumulation, apart from a small initial release, which was taken up again by the end of the experiment.

The carbonate system (TA, pH, and DIC) responded very differently in the Ca- and Mg-free seawater compared to the three other treatments. Although the shape of the response curves were similar, the overall accumulation of alkalinity (ΔTA = 340 ± 14 μmol kg^{-1}) and dissolved inorganic carbon (ΔDIC = 317 ± 11 μmol kg^{-1}) was substantially higher in the ASW-CaMg compared to the other treatments (range ΔTA = 41−69

DOI: 10.1021/acs.est.6b05942
Environ. Sci. Technol. 2017, 51, 3960−3972

μmol kg^{-1} and ΔDIC = 31−66 μmol kg^{-1} in FSW, ASW, and ASW-Ca). The ΔTA and ΔDIC in ASW-CaMg quickly increased over the first 10 days, after which the increase rate slowed down and the accumulation became linear. The long-term accumulation, i.e. between 30 and 137 days, was higher for DIC (168 ± 50 μmol kg^{-1}) than for TA (127 ± 12 μmol kg^{-1}).

The ΔpH showed an "overshoot" response, with a sharp initial increase in the first 5 days, reaching maximum between 4 and 7 days, after which the ΔpH gradually decreased and tended toward an asymptotic equilibrium value at the end of the experiment (Figure 2). Consistent with the stronger alkalinity accumulation in the Ca- and Mg-free seawater, the long-term pH (pH_{t137} minus pH_{t0}) increase was much higher in the Ca- and Mg-free seawater (ΔpH = 0.06), compared to the other three treatments (range in ΔpH = −0.01 to 0.035 at 137 days).

Olivine Dissolution Stoichiometry and Rates. PHREEQC kinetic modeling of the ASW, ASW-Ca, and ASW-CaMg treatments suggested that all reactive fluid media in experiment A3 were undersaturated for forsterite ($\Omega_{forsterite}$ = 10^{-5} for FSW, ASW, and ASW-Ca and $\Omega_{forsterite}$ = 10^{-10} for ASW-CaMg).

The accumulation rates R were determined by the best model fit[23] (see Figure S6 for representative examples) to the response curves of the olivine dissolution products ΔSi, ΔNi, ΔMg, and ΔTA and the ensuing CO_2 sequestration ΔDIC (Table 1). As emphasized above, different dissolution products

Table 1. Release Rate R^i_{max} (μmol kg^{-1} day^{-1}) of Each of the Measured i Variables ΔSi, ΔNi, ΔMg, ΔTA, and ΔDIC within Each Experiment[a]

exp	medium	$R_{\Delta Si}$	$R_{\Delta Ni}$	$R_{\Delta Mg}$	$R_{\Delta TA}$	$R_{\Delta DIC}$
A1	FSW	0.9[1]	0.2[3]		39.9[2]	6.3[2]
A2	FSW	2.8[1]	0.4[2]		52.3[2]	13.6[2]
A3	FSW	0.6[2]	0.1[3]		11.5[2]	7.9[2]
	ASW	0.6[1]	0.2[3]		33[2]	2.1[2]
	ASW-Ca	0.9[1]	0.2[2]		1.6[2]	1.7[2]
	ASW-CaMg	3.8[3]	0.2[3]	35.4[3]	32.4[3]	22.7[3]

[a]The number next to each of the R^i_{max} values corresponds to the model that best fit the data (for the significance of parameters, see the Materials and Methods section), where 1 = linear model, 2 = saturation model, 3 = combined model according to the equations in Table S6.

tended to have different response curves within the same treatment, thus indicating nonstoichiometric dissolution (Table 1). In the case of ΔSi, the accumulation response was generally best described by a linear model (model 1, Table S5), while for ΔTA, ΔDIC, ΔMg, and ΔNi, the profiles were typically best fitted with a saturation model (model 2, Table S5) or a combination of short-term saturation with a long-term linear increase (model 3, Table S5). Only in the ASW-CaMg treatment (experiment A3) could all variables be described best by model 3 (Table S5)

To further illustrate the absence of stoichiometric dissolution in either natural or artificial seawater in the presence of magnesium, Figure S8 plots the accumulation of response variables in experiment A3 normalized for stoichiometry (Table S1: ΔSi/1, ΔTA/4, ΔNi/0.0075, and ΔMg/1.87). Only in the ASW-CaMg treatment did olivine dissolution tend to become stoichiometric, as shown by the similar responses for ΔMg and ΔTA (Figure S8).

Because of nonstoichiometric dissolution, the olivine dissolution rate constant k_i showed a dependence on the response variable (ΔSi, ΔNi, ΔMg, ΔTA, and ΔDIC; Table 2).

Table 2. Olivine Dissolution Constant k_i (μmol m^{-2} day^{-1}) Based on the R^i_{max} (Table 1) of Each of the i Variables ΔSi, ΔNi, ΔMg, ΔTA, and ΔDIC within Each Experiment

exp	solvent	$k_{\Delta Si}$	$k_{\Delta Ni}$	$k_{\Delta Mg}$	$k_{\Delta TA}$	$k_{\Delta DIC}$
A1	FSW	1	31		16	2
A2	FSW	3	56		13	3
A3	FSW	2	60		10	7
	ASW	2	74		28	2
	ASW-Ca	3	65		2	1
	ASW-CaMg	13	65	63	27	19

The rate constant based on ΔNi ($k_{\Delta Ni}$) is the highest of all response variables and is similar across all treatments (31−74 μmol of olivine m^{-2} day^{-1}). In the ASW-CaMg treatment, $k_{\Delta Mg}$ (63 μmol of olivine m^{-2} day^{-1}) was consistent with $k_{\Delta Ni}$ values, while $k_{\Delta Si}$ were an order of magnitude lower than $k_{\Delta Ni}$ values in the reactive fluid media containing Mg^{2+} (Table 1 and 2). The exclusion of Mg^{2+} in the Mg-free reactive fluid (ASW-CaMg) increased $k_{\Delta Si}$ by 1 order of magnitude. The values of both $k_{\Delta TA}$ and $k_{\Delta DIC}$ show substantial variation between treatments, and are highest in the ASW-CaMg treatment. The temperature-normalized[24] (to 25 °C) mean values for k_i (where i = ΔSi, ΔNi, ΔTA, or ΔDIC), for the FSW and ASW cases are shown in Figure 3 (the ASW-Ca and ASW-CaMg treatments are considered unrealistic for ESW and are thus excluded).

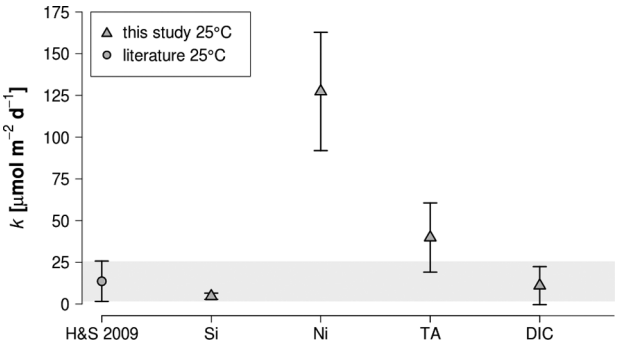

Figure 3. Olivine dissolution rate constant k, calculated as the mean (± SD) value of the different response variables measured in the three agitation experiments A1, A2, and A3 (Table S4). To obtain the most-realistic estimates for olivine dissolution in seawater, only values from the FSW and ASW treatments were considered. For comparison, the estimated value by Hangx and Spiers[14] from previous studies (literature, H&S 2009) is given in the same units as the rates obtained in this study. The literature value and range are denoted by the gray circle and the gray area for clarity. The gray triangles represent the values obtained in this study at 17 °C but recalculated to 25 °C, the same standard temperature as the literature estimates.

SEM−EDX. SEM−EDX analyses of mineral grains from fresh, unreacted olivine were generally angular, with sharp edges (Figure 4A). In contrast, olivine grains that had been rotating during the entire experiment (137 days) were generally subrounded (Figure 4B), suggesting abrasion due to grain−grain collisions. The Mg-to-Si atomic ratios (Mg/Si) at the surface of the unreacted particles were significantly higher (mean ± SEM Mg/Si = 2.11 ± 0.02, n_{grains} = 6; Figure S9) than for grains that were agitated in solution (mean ± SEM Mg/Si

DOI: 10.1021/acs.est.6b05942
Environ. Sci. Technol. 2017, 51, 3960−3972

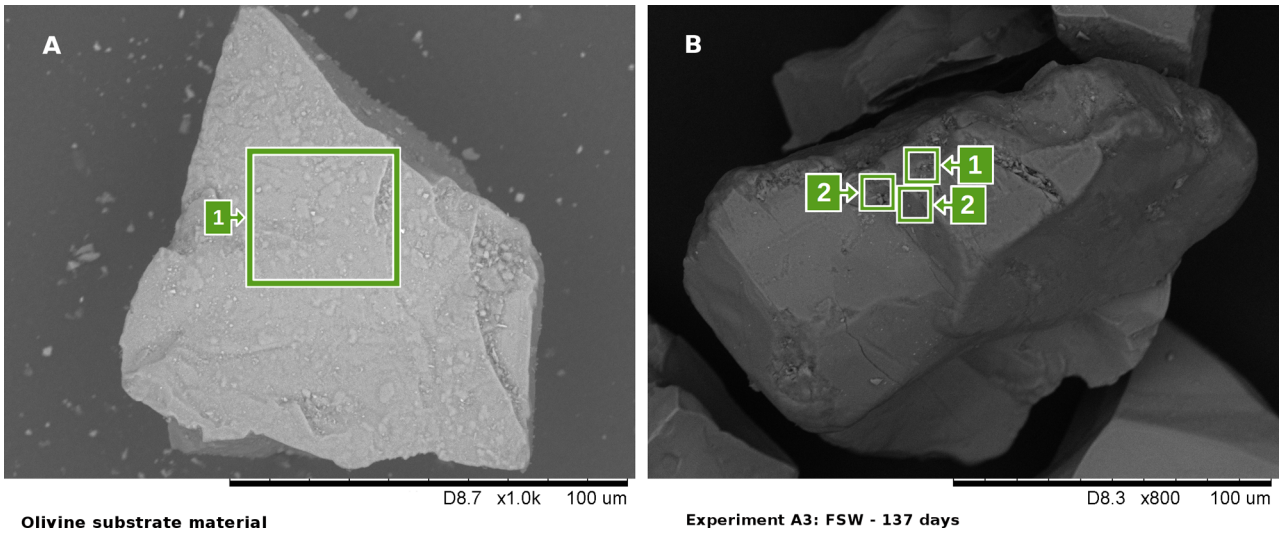

Figure 4. (A) SEM−EDX micrograph of unreacted olivine (substrate material) with very clear angular features and sharp edges. The Mg-to-Si atomic ratio in area 1 typically lies between 2 and 2.5. (B) SEM−EDX micrograph of an olivine particle after being subjected to continuous movement in FSW during 137 days (experiment A3). On the surface of the same olivine particle, abrupt changes in Mg-to-Si atomic ratios can be observed within small distances. Areas denoted with 1 are characterized by Mg-to-Si atomic ratios of 2−2.5, while Mg-to-Si atomic ratios in areas denoted with 2 showed values of around 1. Such locations, where the Mg-to-Si ratio decreases well below 2, are considered local weathering sites.

1.7 ± 0.04−2 ± 0.03, n_{grains} = 3−10; Figure S9). This suggests preferential mobilization of Mg during dissolution, consistent with the higher dissolution rates obtained for Mg and Ni compared to Si. The preferential leaching of Mg^{2+} (lowest Mg-to-Si ratio) was most prominent in the ASW-CaMg treatment (Figure S10), where areas with Mg/Si ≤ 1 and lower were observed. No carbonate minerals were observed on any of the analyzed olivine grains.

Potential for Carbonate Precipitation. The inorganic carbon content (C_{inorg}) in the solid mineral phase recovered from experiment A3 was very low (mean C_{inorg} < 0.005%) and was not significantly different between the four treatments (one-way ANOVA, p = 0.112; Figure S9). Small changes in the solid-phase carbonate content (which are difficult to measure) could nevertheless be associated with substantial changes in the alkalinity of the supernatant. Although not significantly different, the difference in C_{inorg} content between FSW and ASW-CaMg was 0.003 mass percent. If this difference would be real and caused by carbonate precipitation, this would imply that the FSW contained 37 μmol kg^{-1} of $CaCO_3$ in excess to the ASW-CaMg, when expressed per unit volume of fluid. The absence of this precipitation would hence cause the alkalinity to be 74 μmol kg^{-1} higher in ASW-CaMg. However, the measured ΔTA difference between the ASW-CaMg treatment and the FSW and ASW was much higher, amounting to ca. 300 μmol TA kg^{-1} at the end of experiment A3 (Figure 2). Accordingly, carbonate precipitation cannot explain the difference in alkalinity between the FSW and ASW-CaMg treatments, and so it was likely that more olivine dissolution took place in the ASW-CaMg treatment.

DISCUSSION

The dissolution experiments here demonstrate several features regarding olivine weathering in seawater and its potential applications for ESW in coastal settings. First, the basic principle underlying ESW in seawater appears to work. Olivine dissolution in natural seawater under nonsterile laboratory conditions consistently causes alkalinization, followed by CO_2 invasion from the atmosphere into the seawater, at rates in agreement with those estimated by previous studies.[14,24,25] Second, apparent nonstoichiometric dissolution complicates the experimental determination of the rate and extent of olivine dissolution within the seabed, making it more challenging to assess of the efficiency of ESW. Therefore, the quantification of the actual olivine dissolution rate under realistic in situ conditions will require a multiparameter approach, combining flux measurements of dissolved silicate, dissolved metals (nickel and iron), and alkalinity, with appropriate experimental controls. Third, the rate of olivine dissolution within the seabed can be limited by saturation effects, which could decrease the efficiency of ESW applications. Fourthly, the extent to which secondary reactions impact the CO_2 sequestration efficiency of olivine dissolution under in situ conditions remains unresolved and is an important issue to address in further studies on coastal ESW. We will now discuss each of these aspects in more detail.

Quantification of the Olivine Dissolution Rate. To be implemented as a negative emission technology for climate change mitigation,[7] the carbon sequestering potential of marine olivine dissolution needs to be quantified. In other words: How much olivine dissolution occurs within the seabed? What is the time frame in which olivine particles react? How much CO_2 is eventually taken up by the seawater as a consequence of ESW?

The overall CO_2 sequestration rate (R_{CO_2}; mol CO_2 per m^2 of seabed per unit of time) can be expressed as

$$R_{CO_2} = \gamma_{CO_2} \times R_{OLI} = \gamma_{CO_2}(k_{OLI} \times A_{surface} \times C_{OLI}) \quad (1)$$

To determine the effectiveness of coastal ESW, both the factors γ_{CO_2} and R_{OLI} need to be accurately constrained. The CO_2 sequestration efficiency γ_{CO_2} specifies the net amount of CO_2 that is taken up from the atmosphere during the dissolution of 1 kg of olivine within the seafloor (this parameter will be further discussed below). For a given amount of finely ground olivine distributed onto the seafloor (C_{OLI}; mol of olivine m^{-2} of seabed), the olivine dissolution rate (R_{OLI}; mol of olivine per

DOI: 10.1021/acs.est.6b05942
Environ. Sci. Technol. 2017, 51, 3960−3972

m^2 of seabed per unit of time) determines over what time frame the ESW application will be effective (dissolution period $\tau = C_{OLI}/R_{OLI}$). The olivine dissolution rate R_{OLI} further depends on the specific surface area of the mineral grains ($A_{surface}$; m^2 g^{-1}) and the intrinsic dissolution rate constant (k_{OLI}; mol of olivine per m^2 of grain surface area per unit of time).

In practical ESW applications, the olivine dissolution rate (R_{OLI}) within the seabed can be determined experimentally by monitoring the release of olivine dissolution products from the seabed. This poses the question as to which dissolution product (e.g., Mg^{2+}, Si, and TA) should be monitored as a reliable proxy for the olivine dissolution rate in field-type experiments. The use of both dissolved silicate and alkalinity is nontrivial as these are generated in sediments by other processes than olivine dissolution.[26] Any observed sediment efflux of dissolved silicate and alkalinity can thus not be exclusively attributed to olivine dissolution. Furthermore, Mg^{2+} cannot be used as a dissolution proxy due to the high background concentration in seawater (~50 mmol of Mg^{2+} kg^{-1} of seawater), and thus, its accumulation in the overlying water cannot be reliably measured.

Our experiments suggest that Ni^{2+} could be a suitable dissolution proxy, generating a dissolutive accumulation, which substantially supersedes the ambient seawater concentration[27,28] (0.002−0.16 μmol Ni kg^{-1}). This way, pore water accumulation and sediment fluxes of Ni can be accurately measured using standard analytical techniques for trace metals (e.g., inductively coupled plasma−mass spectrometry). However, to qualify as a good proxy for sedimentary dissolution of olivine, two important conditions need to be fulfilled. First, the efflux of the olivine proxy (Ni) from the sediment should also match the release rate of the weathering products in the pore solution. In this regard, Ni^{2+} seems an advantageous proxy. The natural cycling of Ni^{2+} in coastal sediments is restricted, and so the observed Ni^{2+} efflux from the sediment in olivine addition experiments can be fully attributed to olivine dissolution. Still, in future studies, it should be verified whether the Ni^{2+} release is modulated by diagenetic effects within the sediment (e.g., sorption onto minerals).

A second important condition is that stoichiometric dissolution of olivine occurs, so that the Ni^{2+} release can be properly rescaled to the overall olivine dissolution rate R_{OLI} by means of the Ni content of the olivine source rock that is used[25]. However, our experiments suggest that this not the case (Tables 1 and 2). The experiments A1−A3 show that, when assessed over short-time scales, the dissolution of olivine in seawater is nonstoichiometric, implying incongruent dissolution under Earth surface conditions[29]. In the absence of secondary precipitation reactions, nonstoichiometric dissolution cannot continue indefinitely. Experiments of longer time scales should therefore clarify to what extent the Ni^{2+} release from sediments can be a valid proxy for in situ olivine dissolution.

In our dissolution experiments, the k_i value for Si (determined at the initial time t_0) was ca. 30 times lower compared to that of Ni (or Mg). This suggests a preferential release of divalent cations, respective to silicate. The preferential release of metal cations (Ni^{2+} and Mg^{2+}) compared to Si, and the observed quasi-linear increase in ΔSi are typical for solid-state diffusion in silicate minerals,[29] which facilitates the formation of a "surface (altered) layer".[30] The crystal ionic radius of nickel (83 pm) is only slightly smaller than that of magnesium[31] (86 pm), implying that both metal ions will have a similar rate of solid-state diffusion. Both Pokrovsky and Schott[25] and Palandri and Kharaka[22] already suggested that for slightly alkaline solutions (e.g., seawater), forsterite dissolution at steady-state is controlled by the decomposition of a protonated surface complex, which is silica-rich and magnesium-deficient. Maher et al.[32] postulate that olivine dissolution occurs as a series of boundary layer processes, in which primary dissolution of cations is followed by dissolution of silicic acid ions, which may subsequently repolymerize at the surface. This implies that the measured dissolved silica release rate is a net value, which may not serve as the sole proxy for olivine dissolution. Although in some SEM−EDX images -particularly those from the ASW-CaMg treatment (Figure S10), the particle surface did look as if flakes of surface material had been detaching, and the examined olivine grains did not show any evidence of secondary silicate precipitates.[17,33−35]

A significant finding here is that SEM−EDX analyses show decreasing Mg-to-Si atomic ratios of the forsterite surface between initial substrate and reacted material (Figure S9). Rather than a buildup of thick silica formations, these decreasing Mg-to-Si ratios corroborate the mechanism of a cation-leached, surface altered layer formation by preferential dissolution and subsequent repolymerization processes sensu Hellmann et al.[30] and Maher et al.[32] The time scale on which the weathering takes place in this study is much longer than in high-temperature and high-pressure studies or studies in which an elevated pCO_2 is employed.[29] This so-called "unstrained dissolution",[36] combined with physical disturbances, such as grain abrasion, does not allow for the buildup of a conspicuous passivating layer or thick silicate precipitates.

The nonstoichiometric dissolution as observed in the experiments here emphasizes that the proper quantification of olivine dissolution in field-type ESW experiments requires a careful experimental design. Overall, the nonstoichiometric dissolution of olivine makes the experimental assessment of ESW more challenging. One cannot simply measure one dissolution proxy (e.g., Ni^{2+}) and estimate the release of other reaction products by application of reaction stoichiometry. Moreover, both dissolved silicate and alkalinity are generated in sediments by other processes than olivine dissolution.[26] From a biogeochemical perspective, it is crucial to know how olivine dissolution stimulates the efflux of dissolved silicate and alkalinity from the seabed because the efflux of alkalinity is the ultimate driver of CO_2 uptake,[37] while silicate could stimulate primary productivity by marine diatoms. Hence, a multiparameter assessment, combining flux measurements of Ni^{2+}, dissolved silicate, and alkalinity with appropriate experimental controls, seems to provide the best strategy to confidently determine the olivine dissolution rate under in situ conditions.

Impact of Saturation. The values for the dissolution rate constant k of olivine in seawater obtained in this study are consistent with literature values. For the temperature ranges used in FSW and ASW, the dissolution rate constant varied between 1.9 ± 0.8 μmol of olivine m^{-2} day^{-1} for k_{Si} and 56 ± 18 μmol of olivine m^{-2} day^{-1} for k_{Ni} (mean ± SD values). Normalized for temperature differences, these k value ranges corresponded well with the mean value of 14 μmol of olivine m^{-2} day^{-1}, as compiled by Palandri and Kharaka[22] and Hangx and Spiers,[14] of which the latter had an order of magnitude of variation around the mean (Figure 3).

The nonstoichiometric dissolution in the seawater media FSW and ASW, together with the saturation behavior observed in the TA, Mg^{2+}, and Ni^{2+} results (Figure 1), suggest that the

DOI: 10.1021/acs.est.6b05942
Environ. Sci. Technol. 2017, 51, 3960−3972

olivine dissolution approached thermodynamic equilibrium, thus slowing down the reaction. Only by using a lower solubility product for forsterite (log K = 26.448) than those found in the PHREEQC databases did model simulations indeed show a slowing of the dissolution reaction by saturation, mirroring our experimental observations. Furthermore, the DIC accumulation followed that of alkalinity perfectly in all cases, albeit with a time lag. This lag is due to the relatively slow process of CO_2 invasion[38] and is also observed in the pH response, which first increases to reach a maximum and then subsequently decreases again. This pH response reflects the initial removal of protons through olivine dissolution, followed by a replenishment of the proton pool by lagged CO_2 transfer.

The observed time response of the reaction products in our experiments provide a first idea about the possible influence of saturation effects under in situ conditions. Our experiments show that saturation occurs within a time frame of about 20 days (Figures 1 and 2), for an experimental setup with 15 g of olivine in 300 mL of seawater (i.e., 20 mL of solution g^{-1} of olivine). Assuming the same dissolution rate occurs under in situ pore water conditions, the ratio of pore solution to olivine will be lower. For example, if 10−20% of the solid sediment consists of olivine (mixing a 1−2 cm olivine layer into the top 10 cm of sediment) and assuming a porosity of 0.8 and an olivine particle density of 3.3 g mL^{-1}, we obtain a ratio of 6−12 mL of solution g^{-1} of olivine. Based on our results, we determined that such a pore solution will be saturated within 4.5 to 9 days, after which olivine dissolution will slow down and cease. However, the pore water of coastal sediments is also regularly refreshed through physical, advective pore water flow induced by waves and currents[39] and biological irrigation by burrowing macrofauna.[40,41] Coastal sediments subject to moderate and high bioirrigation show flushing rates in the range of 10−100 L m^{-2} day^{-1},[39] implying that the pore solution of the first 10 cm would be refreshed on a time scale of 0.5−8 days (assuming a porosity range from 0.5 to 0.8). In these sediments, irrigation appears sufficient to counteract the saturation of olivine dissolution in the pore water. However, in more cohesive (muddy) coastal sediments with flushing rates <10 L m^{-2} day^{-1}, saturation effects can be expected, which could decrease the efficiency of enhanced olivine weathering applications. Therefore, a judicious choice of the application location seems warranted.[42]

CO_2 Sequestration Efficiency. The experiments in this study were performed in a setup that allowed free gas exchange with the atmosphere, while internal biological processes affecting the DIC pool were excluded (i.e., primary production and microbial degradation of organic matter).[26,37] Accordingly, the observed DIC increase in the experiments can be entirely attributed to CO_2 invasion induced by olivine dissolution, illustrating the proof-of-principle that ESW enhanced silicate weathering works as a NET.

The CO_2 sequestration efficiency expresses the amount of CO_2 transferred across the air−sea interface per unit mass of silicate rock that dissolves within the seabed and can be written as

$$\gamma_{CO_2} \equiv \frac{R_{CO_2}}{R_{OLI}} = \frac{R_{CO_2}}{R_{TA}}\frac{R_{TA}}{R_{OLI}} = (\partial \Sigma CO_2/\partial TA)_{pCO_2}\frac{R_{TA}}{R_{OLI}} \quad (2)$$

This formulation reflects the two consecutive steps in the process of CO_2 sequestration. In a first step, olivine dissolution takes place (rate R_{OLI}), which increases alkalinity in the pore solution (rate R_{TA}). This alkalinity increase will then shift the acid−base equilibrium from dissolved CO_2 to bicarbonate and carbonate, thus stimulating a CO_2 uptake from the atmosphere across the air−sea interface (rate R_{CO_2}).[26,37] The CO_2 sensitivity$(\partial \Sigma CO_2/\partial TA)_{pCO_2}$ specifies how much CO_2 is taken up from the atmosphere for each mole of alkalinity that is released from the seabed. This thermodynamic factor is evaluated at a given partial pressure of CO_2 in the atmosphere and is dependent on the local salinity, temperature, and chemical composition of the coastal seawater.[43] Calculating the CO_2 sensitivity over the entire experimental period, and for all the experiments that had full ionic strength of seawater (A1, A2, A3: FSW and A3: ASW), we obtain a CO_2 sensitivity of 0.84 ± 0.1 (mol of DIC mol^{-1} of TA), which is in close agreement with the theoretical value 0.854 for seawater at the experimental conditions employed (T = 17 °C, S= 33, TA = 2400 μmol L^{-1}, and pCO_2 = 400 ppmv).[44]

Accordingly, the CO_2 uptake in our experiments appears entirely congruent with the standard acid−base thermodynamics of the carbonate system in seawater. Nevertheless, the alkalinity increase during olivine dissolution, R_{TA}/R_{OLI}, was less than expected. Traditionally, olivine dissolution is described by the reaction equation:

$$Mg_{2(1-x)}Fe_{2x}SiO_4 + 4H^+ \rightarrow 2(1-x)Mg^{2+} + 2xFe^{2+} + H_4SiO_4 \quad (3)$$

Because 4 moles of protons are consumed per mole of olivine dissolved, and hence 4 mol of alkalinity are produced, a ratio ($\Delta TA/\Delta Si$ = 4 (R_{TA}/R_{OLI} = 4)) is expected. Only in the ASW-CaMg treatment, the $\Delta TA/\Delta Si$ approached the expected value of 4, while it was substantially less in the FSW, ASW, and ASW-Ca treatments. These observations suggests that the Equation 3 does not provide a complete description of the overall olivine dissolution process, but that secondary reactions could be active. Overall, CO_2 sequestration efficiency can be formulated as

$$\gamma_{CO_2} = 4(\Delta \Sigma CO_2/\Delta TA)(1-x) \quad (4)$$

Here, 4 denotes the theoretical stoichiometry between olivine dissolution and CO_2,[5,14] and x denotes a reduction in the CO_2 sequestration efficiency due to secondary reactions. Because our slurry experiments were conducted with oxygenated seawater, one such possible reaction is the aerobic oxidation of ferrous iron:

$$Fe^{2+} + \frac{1}{4}O_2 + 1\frac{1}{2}H_2O \rightarrow FeOOH + 2H^+ \quad (5)$$

This reoxidation process produces free protons, thus consuming again the alkalinity generated during dissolution of the Fe-component of olivine. The olivine employed here contains 6% of Fe (Table S1), which would reduce the alkalinity release by an equal percentage. However, this reduction is not enough to explain the observed $\Delta TA/\Delta Si$ values. Another possibility to reduce the ΔTA-to-ΔSi ratio is calcium carbonate precipitation:

$$Ca^{2+} + 2HCO_3^- \rightarrow CaCO_3 + CO_2 + H_2O \quad (6)$$

Although the supernatant in the FSW and ASW was saturated with respect to calcite and aragonite, magnesium is known to act as an inhibitor for $CaCO_3$ nucleation in seawater, limiting

DOI: 10.1021/acs.est.6b05942
Environ. Sci. Technol. 2017, 51, 3960−3972

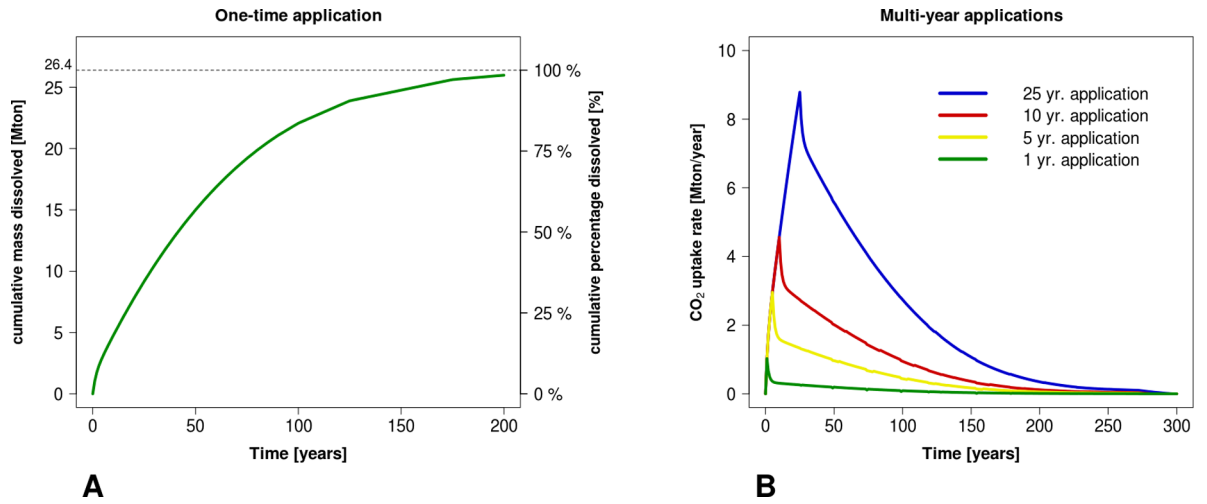

Figure 5. (A) Model results of both absolute and relative cumulative dissolution over time (using dissolution rate constant values as obtained from the experiments in this study) of a one-time hypothetical coastal olivine application of 12 Mm^3, or 26.4 Mton, of olivine sand with the same characteristics as that used here. (B) Model results of the yearly CO_2 uptake rate as a consequence of hypothetical repeated (multiyear) olivine application as a substitute for yearly coastal sand nourishments during periods of 1, 5, 10, and 25 years.

its precipitation[45,46]. Moreover, exclusion of Ca^{2+} and Mg^{2+} from the ASW-CaMg (section 3 of the Supporting Information) implied a strong undersaturation with respect to calcium and magnesium carbonate, thus preventing carbonate precipitation. Additionally, our SEM−EDX analyses did not reveal carbonate minerals on the surface of olivine grains, while at the end of the dissolution experiment, no significant increase in the inorganic carbon (carbonate) content of the solid phase was observed. Accordingly, we consider carbonate precipitation unlikely in the batch experiments performed here, and hence, the cause of the $\Delta TA/\Delta Si < 4$ remains unexplained and requires further investigation.

Thermodynamic modeling in Griffioen[47] suggests that precipitation of the hydrated phyllosilicate sepiolite ($Mg_4Si_6O_{15}(OH)_2{\cdot}6H_2O$) could reduce $\Delta TA/\Delta Si$ values, thus inducing a lower CO_2 sequestration efficiency of enhanced olivine weathering in seawater. However, no sepiolite was found in the XRD analyses. The extent to which secondary reactions impact the CO_2 sequestration efficiency of olivine dissolution under in situ conditions within the seabed remains an important issue to address in further studies on coastal ESW.

Due to the exclusion of Mg^{2+} and Ca^{2+}, the ionic strength of the ASW-CaMg medium was lower than that of the ASW (Table S3). The ionic strength of the ASW was 0.72 mol kg^{-1}, while that of ASW-Ca was 0.015 mol kg^{-1} (or 2%) lower than ASW. Equally, the ionic strength of ASW-CaMg was 0.0975 mol kg^{-1} (or 13%) lower than that of ASW. Ionic strength impacts the activity coefficients of aqueous species and has been found to impact dissolution kinetics, particularly at lower pH.[16] Still, other factors (i.e., pCO_2, pH, and saturation state) exhibit a much larger influence on dissolution kinetics[48,49]. Given the relatively high pH in the reactive fluids (pH 7.9−8.2) and the fact that all solutions were highly undersaturated with respect to fosterite, the impact of the lower ionic strength of the ASW-CaMg was likely to be very small.

The rate at which CO_2 is sequestered due to olivine dissolution in seawater can thus be formulated as the following relation:

$$R_{CO_2} = 4R_{OLI} \times \gamma_{CO_2}(1 - x) \quad (7)$$

Here, 4 denotes the theoretical stoichiometry between olivine dissolution and CO_2,[5,14] R_{OLI} is the olivine dissolution rate, γ_{CO_2} is the reaction efficiency of the CO_2 sequestration in seawater, and x is the molar fraction of Fe in the olivine source material.

Olivine Application in a Coastal Geo-Engineering Framework. To place coastal ESW in a broader perspective, a real-world example illustrates its carbon-capturing potential. The Netherlands is a densely populated, industrialized country, with a GDP of ca. 850 billion USD (2013) and ca. 50% of its surface area below sea level.[50] To protect the coastal region of the country where ca. 60% of the GDP is produced,[51,52] continuous large-scale sand nourishments are needed. Between 2000 and 2010, ca. 12 million m^3 (Mm^3) sand per year have been deployed along The Netherlands' coast, which is expected to increase due to predicted climate change-induced sea level rise[51,52] (https://www.noordzeeloket.nl/en/functions-and-use/surface-mining-and-quarrying/).

In a thought experiment, the sand used in these coastal nourishments is replaced by finely ground olivine, as used in the experiments described here. In a hypothetical one-time application of 12 Mm^3 (≈ 26 Mt) of olivine sand, parameter values for $k_{\Delta TA}$ obtained in our experiments (Table 1) were implemented in the Olsen[53] shrinking core model for olivine carbonation (assuming the measured olivine particle size distribution; see section 2 of the Supporting Information). This model has been previously implemented in ten Berge et al.,[54] describing total mass of olivine weathered and consequential CO_2 captured (section 8 of the Supporting Information). Our simulations showed a cumulative weathering of 4% of the olivine after the first year, 12% after 5 years, 35% after 25 years, 57% after 50 years, and 84% after 100 years (Figure 5A). After 200 years, 98% of the initially applied 12 Mm^3 olivine will be dissolved. These values are in accordance with those presented by Hangx and Spiers,[14] in which 100 μm (median diameter: D_{50}) olivine grains would take >100 years to dissolve.

Making use of the earlier derived relationship, eq 6, with γ_{CO_2} = 0.84 and x = 0.06 as discussed above, the amount of carbon dioxide taken up can be estimated. With annual 12 Mm^3 applications, for periods of 1, 5, 10, and 25 years, the CO_2-

DOI: 10.1021/acs.est.6b05942
Environ. Sci. Technol. 2017, 51, 3960−3972

capturing rate would increase from ca. 2.5 Mton CO_2 $year^{-1}$ to a peak value of ca. 9 Mton CO_2 $year^{-1}$ after 25 years of coastal olivine application (Figure 5B). This would be the equivalent of 5% of The Netherlands' yearly 170 Mton CO_2 emissions (2013 value; http://data.worldbank.org/indicator/). Once the application stops, the remaining olivine will dissolve in about 250 years, with decreasing yearly CO_2 uptake rates (Figure 5B). The long time scale over which ESW is effective has two important implications. First, the process of issuing and validating carbon credits for ESW will need to take into account that CO_2 sequestration is not immediately realized at once but stretched out over a century-scale time window. Second, given the long-lasting effects, any potential ecosystem impacts need to be properly assessed and evaluated upfront in small-scale field trials before large-scale ESW application can start.

Environmental Implications. From an ecological perspective, the potential secondary effects of (large-scale) olivine dissolution are a critical issue. Although dilution processes in marine coastal environments will likely prevent accumulation to toxic levels of dissolution products, it is important (and obligatory in e.g. the European Union) to perform upscaling calculations of dissolution product concentrations and their conceivable effects on the marine ecosystem. The main consequences of forsteritic olivine dissolution are increases in Mg^{2+}, Si, TA, DIC, Fe^{2+}, and Ni^{2+}, and their ecosystem effects should be thoroughly assessed. In addition, the geophysical consequences of olivine distribution in coastal ecosystems should be assessed, such as the increase in suspended particulate matter, sediment pore space clogging and smothering effects due to the higher specific density of olivine. While increases in alkalinity and DIC are a desired effect for climate engineering purposes, the increase in Mg^{2+} is not expected to pose a significant threat because of the high background concentration in seawater. Increases in dissolved Si and dissolved Fe can stimulate primary production and thus lead to additional CO_2 sequestration, as recently assessed by model analysis[55]. However, the ultimate impacts on coastal foodwebs of fertilizing by olivine dissolution are uncertain and need further investigation.

The impact of increased nickel flux on marine ecosystems is a matter of potential concern, and has only been scarcely touched upon. Nickel leaches from the olivine mineral matrix in its ionic Ni(II) form. Dissolved nickel occurs in trace concentrations in seawater (0.03−0.16 μmol kg^{-1};[27]), as low as 0.002−0.006 μmol kg^{-1} in the central southern North Sea and up to 0.04 μmol kg^{-1} in the Rhine delta area.[28] In comparison, background nickel concentrations in the control treatments ranged between 0.14 μmol kg^{-1} in the FSW in experiment A3 and 0.45 μmol kg^{-1} in experiment A1, while background Ni concentrations in the artificial seawater media in experiment A3 (ASW, ASW-Ca, and ASW-CaMg) were an order of magnitude lower, between 0.017 and 0.032 μmol kg^{-1}.

The ecotoxicology of nickel in marine organisms and ecosystems is summarized on the Web site of the UK Marine Special Areas of Conservation (http://www.ukmarinesac.org.uk/) and established for the UK at a chronic concentration of 0.25 μmol L^{-1}. Nickel toxicity has been reported in a number of cases:[56−58] negative effects on spawning in mysiid shrimps at 2.4 μmol L^{-1}, DNA damage with associated physiological and cytotoxic effects in the blue mussel *Mytilus edulis* at 0.3 μmol L^{-1}, disrupting ionoregulatory functions in the green crab *Carcinus maenas* between 8.5 and 51 μmol L^{-1} in very low-salinity seawater (0.006 PSU), and organ oxidative stress in the killifish *Fundulus heteroclitus*, also mainly in freshwater. However, one of the conclusions of Blewett et al.[57] and Blewett and Wood[58] is that higher, seawater-like salinities (e.g., 30−38) seem to be negatively correlated with Ni-induced effects. In general, higher salinities are inversely correlated with Ni^{2+} seawater concentrations.[59] Although bioaccumulation of nickel in individual organisms occurs, there seems to be little evidence of biomagnification throughout (marine) foodwebs,[27] although Kumblad et al.[60] present results that suggest the contrary. The potential toxicity of nickel, combined with rather large uncertainties about the magnitude and direction of its response effects, make it paramount to further investigate its ecotoxicological effects within the framework of large-scale application of olivine in coastal environments.

Containment is not an issue for ESW. Before any field-scale application, there should be proper field trials in quasi-contained conditions, such as mesocosm setups, which can be upscaled in, e.g., tidal harbor basins. In the case that a mesoscale field trial (~100 m^2) would be undertaken, common dredging equipment would be used to apply the olivine into the (coastal) environment. The same equipment and expertise can be used to remove the olivine sand, should any acute unforeseen situation develop.

The CO_2 sequestration induced by ESW is governed by the acid−base thermodynamics of seawater, which are well-understood,[26,37,38] therefore rendering the containment of CO_2 in the ocean highly predictable. The central premise of ESW is that it increases the ocean's alkalinity, enabling more CO_2 to be dissolved into seawater at any given pCO_2 compared to the situation in which no alkalinity is added to the ocean. This CO_2 will be stay dissolved in the ocean (or contained) as long as no other process changes the alkalinity of the ocean. In the ESW, the CO_2 storage reservoir (the ocean) is an open system, as CO_2 can be freely exchanged between atmosphere and ocean across the air−sea interface. Because leakage cannot occur in an open system, storage of CO_2 in the ocean is therefore leakage-proof. The evidence that CO_2 will be contained for long periods of time is given by observations on the long-term (>1000 year) carbon cycle and the impact of natural silicate weathering: the long-term fate of fossil CO_2 is to be absorbed in the ocean.[61]

If ESW is applied to coastal systems in a geo-engineering framework, it will be crucial to determine in situ olivine dissolution rates to determine the efficiency of the method.[42] Once in the natural sediment, the olivine will be subject to very different biogeochemical and geophysical conditions. Microbial mineralization processes could greatly increase the CO_2 concentration in the sediment's pore waters,[62] while benthic macrofauna process vast quantities of sediment for their sustenance and mobility.[63,64] These processes are likely to speed up the dissolution process within marine sediments. Large-scale sediment transport and wave action are expected to cause constant particle abrasion and faster mechanical weathering, in turn facilitating faster chemical weathering. If ESW is ever to be applied in a geo-engineering framework, it is of paramount importance to investigate the effects of all of these natural processes on the dissolution of olivine in coastal environments.

DOI: 10.1021/acs.est.6b05942
Environ. Sci. Technol. 2017, 51, 3960−3972

■ ASSOCIATED CONTENT

Supporting Information

The Supporting Information is available free of charge on the ACS Publications website at DOI: 10.1021/acs.est.6b05942.

Experimental details of olivine solution, composition of minerals and media, overview of experimental conditions, calculation of rate constants, model simulations, accumulation of reaction products, solid-phase analysis, and calculation of total mass of olivine weathered and CO_2 captured. (PDF)

■ AUTHOR INFORMATION

Corresponding Author

*E-mail: montserrat@usp.br, f.montserrat@gmail.com.

ORCID

Francesc Montserrat: 0000-0002-9882-3376

Present Address

F.M.: Department of Marine Ecology, Management and Conservation, Institute for Oceanography, University of São Paulo, Praça do Oceanografico 191, 05508-120, São Paulo (SP), Brazil.

Notes

The authors declare no competing financial interest.

■ ACKNOWLEDGMENTS

The authors thank Steven Way, Yvonne van der Maas, Jurian Brasser, and Peggy Bartsch for their contributions and work in the lab. Diana Vasquez is thanked for the many constructive discussions on the manuscript. Jens Hartmann is supported by the German Science Foundation DFG (Exc 177 and HA 4471/10-2). Pol Knops was supported by Deltares Foundation and by the EU climate innovation programme C-KIC, EIT Grant 1.2.1 NMSO. The authors thank the Hercules Foundation (Belgium) for financing the ICP-SF-MS instrument (UABR/11/010). Filip J.R. Meysman was financially supported by the European Research Council (ERC Grant 306933). We thank Vanessa of V. Gonzalez Ortiz Scientific Illustration & Outreach (http://vgonzalezortiz.com/en/) for the TOC art illustration and other graphic advice and services. This research was part of the olivine vs. ocean acidification (OLIvOA) research initiative (http://www.olivoa.eu).

■ ABBREVIATIONS

ESW	enhanced silicate weathering
OA	ocean acidification
OLI	olivine treatment
QUA	quartz treatment
FSW	filtered seawater
ASW	artificial seawater
ASW-Ca	artificial seawater without calcium
ASW-CaMg	artificial seawater without calcium and magnesium
PSU	practical salinity units

■ REFERENCES

(1) Comittee on Geoengineering Climate; Board on Atmospheric Sciences and Climate; Ocean Studies Board; Division on Earth and Life Studies. *Climate Intervention: Carbon Dioxide Removal and Reliable Sequestration*; National Research Council: Washington DC, 2015.

(2) Gasser, T.; Guivarch, C.; Tachiiri, K.; Jones, C. D.; Ciais, P. Negative emissions physically needed to keep global warming below 2 °C. *Nat. Commun.* **2015**, *6*, 7958.

(3) Sanderson, B. M.; O'Neill, B. C.; Tebaldi, C. What would it take to achieve the Paris temperature targets? *Geophys. Res. Lett.* **2016**, *43* (13), 7133−7142.

(4) UNFCCC. *The 2015 Paris Climate Change Conference: COP21.*; 2016; Vol. *99*, pp 97−104.

(5) Schuiling, R. D.; Krijgsman, P. Enhanced Weathering: An Effective and Cheap Tool to Sequester CO2. *Clim. Change* **2006**, *74* (1−3), 349−354.

(6) Hartmann, J.; West, J. A.; Renforth, P.; Köhler, P.; De La Rocha, C. L.; Wolf-Gladrow, D. A.; Dürr, H. H.; Scheffran, J. Enhanced chemical weathering as a geoengineering strategy to reduce atmospheric carbon dioxide, supply nutirents, and mitigate ocean acidification. *Rev. Geophys.* **2013**, *51* (2), 113−149.

(7) The Royal Society. *Geoengineering the climate: science, governance and uncertainty*; The Royal Society: London, United Kingdom, 2009; Vol. *12*.

(8) IPCC. *Climate Change 2014: Synthesis Report. Contribution of Working Groups I, II and III to the Fifth Assessment Report of the Intergovernmental Panel on Climate Change*; IPCC: Geneva, Switzerland, 2014.

(9) Taylor, L. L.; Quirk, J.; Thorley, R. M. S.; Kharecha, P. A.; Hansen, J.; Ridgwell, A.; Lomas, M. R.; Banwart, S. A.; Beerling, D. J. Enhanced weathering strategies for stabilizing climate and averting ocean acidification. *Nat. Clim. Change* **2015**, *6* (4), 402−406.

(10) Ebelmen, J. J. Sur les produits de la décomposition des espècesminérales de la famille des silicates. *Ann. DES MINES* **1845**, *7*, 3−66.

(11) Renforth, P. The potential of enhanced weathering in the UK. *Int. J. Greenhouse Gas Control* **2012**, *10*, 229−243.

(12) Köhler, P.; Hartmann, J.; Wolf-Gladrow, D. A. Geoengineering potential of artificially enhanced silicate weathering of olivine. *Proc. Natl. Acad. Sci. U. S. A.* **2010**, *107* (47), 20228−20233.

(13) Köhler, P.; Abrams, J. F.; Völker, C.; Hauck, J.; Wolf-Gladrow, D. A. Geoengineering Impact of Open Ocean Dissolution of Olivine on Atmospheric CO2, Surface Ocean pH and Marine Biology. *Environ. Res. Lett.* **2013**, *8* (1), 014009.

(14) Hangx, S. J. T.; Spiers, C. J. Coastal spreading of olivine to control atmospheric CO2 concentrations: A critical analysis of viability. *Int. J. Greenhouse Gas Control* **2009**, *3* (6), 757−767.

(15) Wogelius, R. A.; Walther, J. V. Olivine dissolution at 25° C: Effects of pH, CO2, and organic acids. *Geochim. Cosmochim. Acta* **1991**, *55* (4), 943−954.

(16) Pokrovsky, O. S.; Schott, J. Kinetics and mechanism of forsterite dissolution at 25°C and pH from 1 to 12. *Geochim. Cosmochim. Acta* **2000**, *64* (19), 3313−3325.

(17) Oelkers, E. H. An experimental study of forsterite dissolution rates as a function of temperature and aqueous Mg and Si concentrations. *Chem. Geol.* **2001**, *175* (3−4), 485−494.

(18) Rosso, J. J.; Rimstidt, D. J. A high resolution study of forsterite dissolution rates. *Geochim. Cosmochim. Acta* **2000**, *64* (5), 797−811.

(19) ASTM International. Standard Practice for the Preparation of Substitute Ocean Water; *D 1141 - 98*; ASTM International: West Conshohocken, PA, 1999; pp 98−100.

(20) Nieuwenhuize, J.; Maas, Y. E.; Middelburg, J. J. Rapid analysis of organic carbon and nitrogen in particulate materials. *Mar. Chem.* **1994**, *45* (3), 217−224.

(21) Milne, A.; Landing, W.; Bizimis, M.; Morton, P. Determination of Mn, Fe, Co, Ni, Cu, Zn, Cd and Pb in seawater using high resolution magnetic sector inductively coupled mass spectrometry (HR-ICP-MS). *Anal. Chim. Acta* **2010**, *665*, 200−207.

(22) Palandri, J. L.; Kharaka, Y. K. *A compilation of rate parameters of water-mineral interaction kinetics for application to geochemical modeling*; USGS: Menlo Park, CA, 2004; Vol. *2004−1068*.

(23) R Development Core Team. *R: A language and environment for statistical computing*; R Foundation for Statistical Computing: Vienna, Austria, 2008.

DOI: 10.1021/acs.est.6b05942
Environ. Sci. Technol. 2017, 51, 3960−3972

(24) Wogelius, R. A.; Walther, J. V. Olivine dissolution kinetics at near-surface conditions. *Chem. Geol.* **1992**, *97* (1−2), 101−112.
(25) Pokrovsky, O. S.; Schott, J. Forsterite surface composition in aqueous solutions: A combined potentiometric, electrokinetic, and spectroscopic approach. *Geochim. Cosmochim. Acta* **2000**, *64* (19), 3299−3312.
(26) Wolf-Gladrow, D. A.; Zeebe, R. E.; Klaas, C.; Körtzinger, A.; Dickson, A. G. Total alkalinity: The explicit conservative expression and its application to biogeochemical processes. *Mar. Chem.* **2007**, *106* (1−2), 287−300.
(27) WHO. *Environmental Health Criteria No. 108 Nickel*; WHO: Geneva, Switzerland, 1991.
(28) Burton, J. D.; Althaus, M.; Millward, G. E.; Morris, A. W.; Statham, P. J.; Tappin, A. D.; Turner, A. Processes influencing the fate of trace metals in the North Sea. In *Understanding the North Sea system*; Charnock, H., Dyer, K. R., Huthnance, J. M., Liss, P. S., Simpson, J. H., Tett, P. B., Eds.; Springer Science+Business Media: Dordrecht, The Netherlands, 1994; pp 179−190.
(29) Wolff-Boenisch, D.; Wenau, S.; Gislason, S. R.; Oelkers, E. H. Dissolution of basalts and peridotite in seawater, in the presence of ligands, and CO2: Implications for mineral sequestration of carbon dioxide. *Geochim. Cosmochim. Acta* **2011**, *75* (19), 5510−5525.
(30) Hellmann, R.; Wirth, R.; Daval, D.; Barnes, J. P.; Penisson, J. M.; Tisserand, D.; Epicier, T.; Florin, B.; Hervig, R. L. Unifying natural and laboratory chemical weathering with interfacial dissolution-reprecipitation: A study based on the nanometer-scale chemistry of fluid-silicate interfaces. *Chem. Geol.* **2012**, *294−295*, 203−216.
(31) Shannon, R. D. Revised effective ionic radii and systematic studies of interatomic distances in halides and chalcogenides. *Acta Crystallogr., Sect. A: Cryst. Phys., Diffr., Theor. Gen. Crystallogr.* **1976**, *32* (5), 751−767.
(32) Maher, K.; Johnson, N. C.; Jackson, A.; Lammers, L. N.; Torchinsky, A. B.; Weaver, K. L.; Bird, D. K.; Brown, G. E. A spatially resolved surface kinetic model for forsterite dissolution. *Geochim. Cosmochim. Acta* **2016**, *174*, 313−334.
(33) Bearat, H.; McKelvy, M. J.; Chizmeshya, A. V. G.; Gormley, D.; Nunez, R.; Carpenter, R. W.; Squires, K.; Wolf, G. H. Carbon sequestration via asueous olivine mineral carbonation: role of passivating layer formation. *Environ. Sci. Technol.* **2006**, *40* (15), 4802−4808.
(34) Olsson, J.; Bovet, N.; Makovicky, E.; Bechgaard, K.; Balogh, Z.; Stipp, S. L. S. Olivine reactivity with CO2 and H2O on a microscale: Implications for carbon sequestration. *Geochim. Cosmochim. Acta* **2012**, *77*, 86−97.
(35) Garcia, B.; Beaumont, V.; Perfetti, E.; Rouchon, V.; Blanchet, D.; Oger, P.; Dromart, G.; Huc, a.-Y.; Haeseler, F. Experiments and geochemical modelling of CO2 sequestration by olivine: Potential, quantification. *Appl. Geochem.* **2010**, *25* (9), 1383−1396.
(36) Schott, J.; Brantley, S.; Crerar, D.; Guy, C.; Borcsik, M.; Willaime, C. Dissolution kinetics of strained calcite. *Geochim. Cosmochim. Acta* **1989**, *53* (2), 373−382.
(37) Zeebe, R. E.; Wolf-Gladrow, D. A. *CO_2 in Seawater: Equilibrium, Kinetics, Isotopes*; Elsevier Science BV: Amsterdam, The Netherlands, 2001.
(38) Sarmiento, J. L.; Gruber, N. *Ocean Biogeochemical Dynamics*; Princeton University Press: Princeton, NJ, 2006.
(39) Huettel, M.; Berg, P.; Kostka, J. E. Benthic Exchange and Biogeochemical Cycling in Permeable Sediments. *Annu. Rev. Mar. Sci.* **2014**, *6*, 23−51.
(40) Aller, R. C.; Aller, J. Y. The effect of biogenic irrigation intensity and solute exchange on diagenetic reaction rates in marine sediments. *J. Mar. Res.* **1998**, *56* (4), 905−936.
(41) Rao, A. M. F.; Malkin, S. Y.; Montserrat, F.; Meysman, F. J. R. Alkalinity production in intertidal sands intensified by lugworm bioirrigation. *Estuarine, Coastal Shelf Sci.* **2014**, *148*, 36−47.
(42) Meysman, F. J. R.; Montserrat, F. Negative CO_2 emissions via enhanced silicate weathering in coastal environments. *Biol. Lett.* **2017**, *13*, 20160905.
(43) Hofmann, A. F.; Middelburg, J. J.; Soetaert, K.; Meysman, F. J. R. pH modelling in aquatic systems with time-variable acid-base dissociation constants applied to the turbid, tidal Scheldt estuary. *Biogeosciences* **2009**, *6* (8), 1539−1561.
(44) Hofmann, A. A. F.; Soetaert, K.; Meysman, F. J. R. *AquaEnv - an integrated development toolbox for aquatic chemical model generation*; R Foundation for Statistical Computing: Vienna, Austria, 2012
(45) Berner, R. A. The role of magnesium in the crystal growth of calcite and aragonite from sea water. *Geochim. Cosmochim. Acta* **1975**, *39* (4), 489−504.
(46) Karoui, H.; Korchef, A.; Tlili, M. M.; Mosrati, H.; Gil, O.; Mosrati, R.; Ben Amor, M. Effects of Mg2+, Ca2+ and SO42- ions on the precipitation kinetics and microstructure of aragonite. *Ann. Chim.* **2008**, *33* (2), 123−134.
(47) Griffioen, J. Enhanced weathering of olivine in seawater: The efficiency as revealed by thermodynamic scenario analysis. *Sci. Total Environ.* **2017**, *575*, 536−544.
(48) Krevor, S. C. M.; Lackner, K. S. Enhancing serpentine dissolution kinetics for mineral carbon dioxide sequestration. *Int. J. Greenhouse Gas Control* **2011**, *5* (4), 1073−1080.
(49) Giammar, D. E.; Bruant, R. G.; Peters, C. A. Forsterite dissolution and magnesite precipitation at conditions relevant for deep saline aquifer storage and sequestration of carbon dioxide. *Chem. Geol.* **2005**, *217* (3−4), 257−276.
(50) UNESCO World Water Assessment Programme. *The UN World Water Development Report 3: Water in a Changing World*; UNESCO: Paris, London, 2009.
(51) Mulder, J. P. M. *Zandverliezen in het Nederlandse kustysteem; Advies voor Dynamisch Handhaven in de 21e eeuw (in Dutch)*; The Hague: The Netherlands, 2000.
(52) Mulder, J. P. M.; Hommes, S.; Horstman, E. M. Implementation of coastal erosion management in the Netherlands. *Ocean Coast. Manag.* **2011**, *54*, 888−897.
(53) Olsen, A. A. Forsterite dissolution kinetics: Applications and implications for chemical weathering; Virginia State University: Petersburg, VA, 2007.
(54) ten Berge, H. F. M.; van der Meer, H. G.; Steenhuizen, J. W.; Goedhart, P. W.; Knops, P.; Verhagen, J. Olivine Weathering in Soil, and Its Effects on Growth and Nutrient Uptake in Ryegrass (Lolium perenne L.): A Pot Experiment. *PLoS One* **2012**, *7* (8), e42098.
(55) Hauck, J.; Köhler, P.; Wolf-Gladrow, D.; Völker, C. Iron fertilisation and century-scale effects of open ocean dissolution of olivine in a simulated CO_2 removal experiment. *Environ. Res. Lett.* **2016**, *11* (2), 024007.
(56) Millward, G. E.; Kadam, S.; Jha, A. N. Tissue-specific assimilation, depuration and toxicity of nickel in Mytilus edulis. *Environ. Pollut.* **2012**, *162*, 406−412.
(57) Blewett, T. A.; Glover, C. N.; Fehsenfeld, S.; Lawrence, M. J.; Niyogi, S.; Goss, G. G.; Wood, C. M. Making sense of nickel accumulation and sub-lethal toxic effects in saline waters: Fate and effects of nickel in the green crab, Carcinus maenas. *Aquat. Toxicol.* **2015**, *164*, 23−33.
(58) Blewett, T. A.; Wood, C. M. Salinity-Dependent Nickel Accumulation and Oxidative Stress Responses in the Euryhaline Killifish (Fundulus heteroclitus). *Arch. Environ. Contam. Toxicol.* **2015**, *68* (2), 382−394.
(59) CEFAS. *Monitoring and surveillance of non-radioactive contaminants in the aquatic environment and activities regulating the disposal of wastes at sea, 1994*; CEFAS: Lowestoft, England, 1997.
(60) Kumblad, L.; Bradshaw, C.; Gilek, M. Bioaccumulation of 51Cr, 63Ni and 14C in Baltic Sea benthos. *Environ. Pollut.* **2005**, *134* (1), 45−56.
(61) Archer, D. Fate of fossil fuel CO2 in geologic time. *J. Geophys. Res.* **2005**, *110*, 6.
(62) Burdige, D. J. *Geochemistry of Marine Sediments*; Princeton University Press: Princeton, NJ, 2006.
(63) Meysman, F. J. R.; Middelburg, J. J.; Heip, C. H. R. Bioturbation: a fresh look at Darwin's last idea. *TRENDS Ecol. Evol.* **2006**, *21* (12), 688−695.

DOI: 10.1021/acs.est.6b05942
Environ. Sci. Technol. 2017, 51, 3960−3972

(64) Montserrat, F.; Van Colen, C.; Degraer, S.; Ysebaert, T.; Herman, P. M. J. Benthic community-mediated sediment dynamics. *Mar. Ecol.: Prog. Ser.* **2008**, *372* (1), 43−59.

DOI: 10.1021/acs.est.6b05942
Environ. Sci. Technol. 2017, 51, 3960−3972